

Computational Considerations for a Spacecraft Attitude Control System Employing Control Moment Gyros

Bruce K. Colburn*

Texas A&M University, College Station, Texas

and

Larry R. White†

Southern Company Services, Inc., Birmingham, Ala.

Techniques for on-line computation of the steady-state solution of a matrix Riccati equation are studied with respect to speed and accuracy for a class of Control Moment Gyro (CMG) spacecraft attitude control laws. A sensitivity analysis is then performed to investigate the effect of eliminating certain gain term computations so as to reduce the on-line computational burden. Numerical results are provided to indicate the results of the study.

I. Introduction

IN this paper the steady-state matrix Riccati equation is studied with respect to sensitivity and computational burden for a linear regulator controller for spacecraft. The class of systems studied use control moment gyros (CMG's) as the torque driver.¹⁻³ The form of the spacecraft-CMG equation coupling is shown to result in a multi-input, multi-output problem formulation so the tools of linear systems theory can be applied. A feedback policy is determined using the state variable approach and optimal control theory. The development of this control policy utilized Kalman's work showing that the optimal law for the nonlinear system can be given by the solution of the optimization problem for a set of system equations linearized about the current operating point.⁴

When it is desired or necessary to use a full total optimal linear regulator such as in this paper, computational considerations of an on-board control and guidance package become important due to the limited speed and storage

not fine pointing units and they require an exhaustible supply of cold gas.

II. Control Law Formulation

For the conventional SIXPAC CMG configuration, the equations of motion of the vehicle-CMG combination can be written as

$$\dot{\Omega} = J^{-1}[D\delta + E\Omega - \Omega \times J \cdot \Omega + T_{ex}] \quad (1)$$

where

- T_{ex} = the external torque applied to the vehicle
- J = the inertia dyadic of the vehicle-CMG combination
- D = 3×6 time-varying rotation matrix representative of the vehicle orientation, given in Eq. (2)
- E = 3×3 matrix whose elements consist of a combination of time-varying vehicle angular momentum terms
- Ω = 3 vector of total spacecraft angular velocity in spacecraft coordinates

$$D = H_0 \begin{bmatrix} -S\delta_{3(1)}C\delta_{1(1)} & -C\delta_{3(1)}S\delta_{1(1)} & -C\delta_{3(2)}C\delta_{1(2)} & S\delta_{3(2)}S\delta_{1(2)} & 0 & C\delta_{1(3)} \\ 0 & C\delta_{1(1)} & -S\delta_{3(2)}C\delta_{1(2)} & -C\delta_{3(2)}S\delta_{1(2)} & -C\delta_{3(3)}C\delta_{1(3)} & S\delta_{3(3)}S\delta_{1(3)} \\ -C\delta_{3(1)}C\delta_{1(1)} & S\delta_{3(1)}C\delta_{1(1)} & 0 & C\delta_{1(2)} & -S\delta_{3(3)}C\delta_{1(3)} & -C\delta_{3(3)}S\delta_{1(3)} \end{bmatrix} \quad (2)$$

capabilities of space computers, as well as the large number of state equations which can arise. There are other approaches to developing steering laws, however, as shown in Ref. 5.

The system discussed in this paper is a special case of that in Ref. 6. Here the CMG's are considered to be free of gimbal stops and the problem of antiparallel orientations is not considered. Using this approach a control law is developed which is closed-loop and which generates six gimbal rate commands as a linear combination of vehicle attitude and attitude rate. In practice, with large space vehicles, a combination of CMG's and cold gas reaction control jets (RCJ's)⁷ are used, the RCJ's supplying and opposing control torque when the CMG's approach their respective gimbal stops and must be "unwound." However, the RCJ's are only used momentarily and are not the primary means of stabilization as they are

$$E = \begin{bmatrix} 0 & H_z & -H_y \\ -H_z & 0 & H_x \\ H_y & -H_x & 0 \end{bmatrix} \quad (3)$$

$$\delta^T = [\delta_{3(1)}\delta_{1(1)}\delta_{3(2)}\delta_{1(2)}\delta_{3(3)}\delta_{1(3)}] \quad (4)$$

In Eq. (2), $S(x)$ and $C(x)$ refers to sine and cosine of (x) , and H_0 is the angular momentum available per CMG. The gimbal angle $\delta_{i(j)}$ notation refers to the i th gimbal of the j th CMG of the SIXPAC configuration shown in Fig. 1. The steering laws are concerned with commanding CMG gimbal rates that will cause the moment exerted on the vehicle by the CMG's to reproduce the commanded torque as nearly as possible. The basic attitude control configuration studied is shown in Fig. 2.

When the primary external torque is due to gravity gradients, it is shown in Ref. 8 that this torque can be expressed as

$$T_{ex} = T_n(t) + G(t)\theta \quad (5)$$

Presented as Paper 76-157 at the AIAA 14th Aerospace Sciences Meeting, Washington, D. C., Jan. 26-28, 1976; submitted Dec. 12, 1975; revision received Oct. 7, 1976.

Index category: Spacecraft Attitude Dynamics and Control.

*Assistant Professor, Department of Electrical Engineering. Member AIAA.

†Power Engineer.

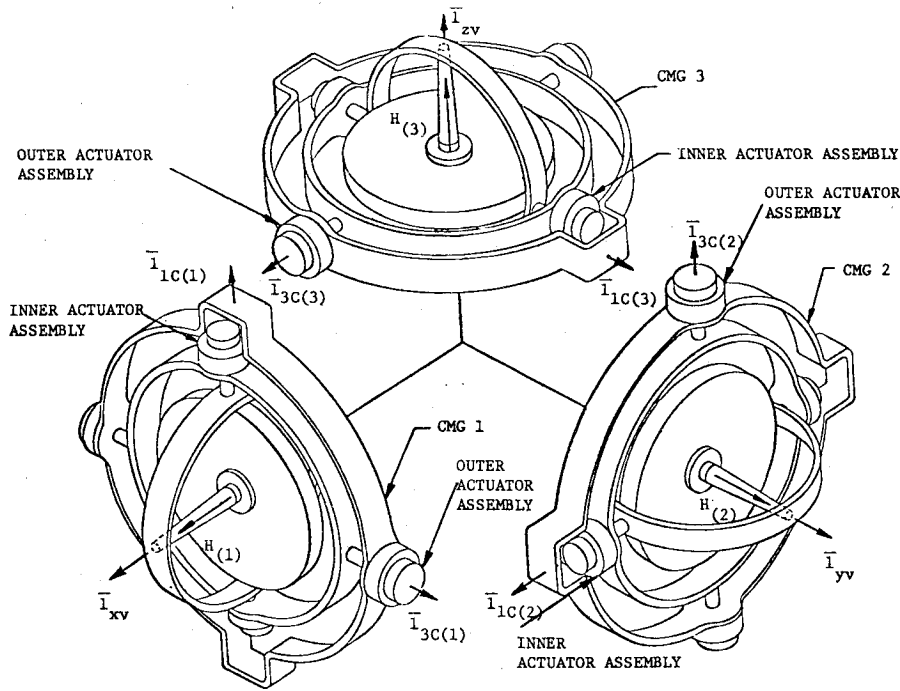


Fig. 1 Conventional CMG SIXPAC configuration.

where

$T_n(t)$ = a time dependent gravity gradient torque evaluated at a nominal attitude

$\theta = \theta_1, \theta_2, \theta_3$; Euler angles corresponding to the $x-y-z$ vehicle axes

$$G = \left. \frac{\partial T_n(t)}{\partial \theta} \right|_{\theta=\theta_{\text{nominal}}}$$

The components of the body rates can be related to the Euler angle rates by manipulating the transformation from inertial space to vehicle space. If the Euler sequence of rotations is 1, 2, 3, then the vehicle reference frame (v) may be related to the inertial reference frame (z) as

$$v = \theta z = [3_\theta][2_\theta][1_\theta]z \quad (6)$$

$$1_\theta = \begin{bmatrix} 1 & 0 & 0 \\ 0 & \cos\theta_1 & \sin\theta_1 \\ 0 & -\sin\theta_1 & \cos\theta_1 \end{bmatrix} \quad (7a)$$

$$2_\theta = \begin{bmatrix} \cos\theta_2 & 0 & -\sin\theta_2 \\ 0 & 1 & 0 \\ \sin\theta_2 & 0 & \cos\theta_2 \end{bmatrix} \quad (7b)$$

$$3_\theta = \begin{bmatrix} \cos\theta_3 & \sin\theta_3 & 0 \\ -\sin\theta_3 & \cos\theta_3 & 0 \\ 0 & 0 & 1 \end{bmatrix} \quad (7c)$$

are unitary matrices. Through an involved series of transformations⁸ the Euler and vehicle rates can be related by

$$\begin{bmatrix} \dot{\theta}_1 \\ \dot{\theta}_2 \\ \dot{\theta}_3 \end{bmatrix} = \begin{bmatrix} \cos\theta_3/\cos\theta_2 & -\sin\theta_3/\cos\theta_2 & 0 \\ \sin\theta_3 & \cos\theta_3 & 0 \\ -\tan\theta_2\cos\theta_3 & \tan\theta_2\sin\theta_3 & 1 \end{bmatrix} \begin{bmatrix} \Omega_1 \\ \Omega_2 \\ \Omega_3 \end{bmatrix} \quad (8)$$

Equations (1) and (8) represent the basic dynamics of the system to be controlled. The state variables are defined to be

$$\begin{bmatrix} x_1 \\ x_2 \\ x_3 \end{bmatrix} = \begin{bmatrix} \theta_1 \\ \theta_2 \\ \theta_3 \end{bmatrix} = \theta \quad (9)$$

$$\begin{bmatrix} x_4 \\ x_5 \\ x_6 \end{bmatrix} = \begin{bmatrix} \Omega_1 \\ \Omega_2 \\ \Omega_3 \end{bmatrix} = \Omega \quad (10)$$

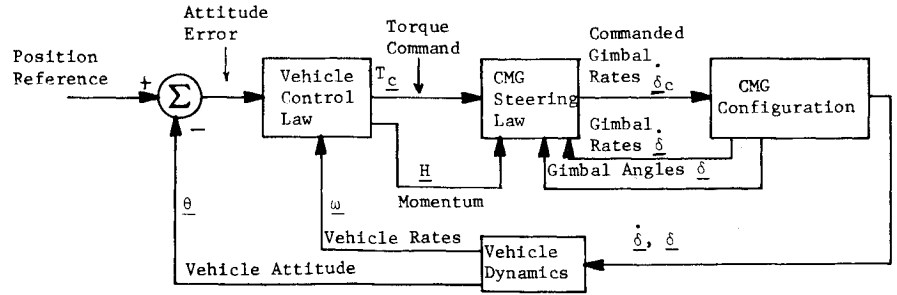
and

$$\begin{bmatrix} x_7 \\ x_8 \\ x_9 \\ x_{10} \\ x_{11} \\ x_{12} \end{bmatrix} = \begin{bmatrix} \delta_{1(1)} \\ \delta_{1(2)} \\ \delta_{1(3)} \\ \delta_{3(1)} \\ \delta_{3(2)} \\ \delta_{3(3)} \end{bmatrix} = \delta \quad (11)$$

the gimbal rates are chosen as the control vector so that

$$\begin{bmatrix} u_1 \\ u_2 \\ u_3 \\ u_4 \\ u_5 \\ u_6 \end{bmatrix} = \begin{bmatrix} \dot{\delta}_{1(1)} \\ \dot{\delta}_{1(2)} \\ \dot{\delta}_{1(3)} \\ \dot{\delta}_{3(1)} \\ \dot{\delta}_{3(2)} \\ \dot{\delta}_{3(3)} \end{bmatrix} = \dot{\delta} \quad (12)$$

Fig. 2 Basic CMG steering law configuration.



Using Eqs. (8-12), the state equations become

$$\begin{bmatrix} \dot{x}_1 \\ \dot{x}_2 \\ \dot{x}_3 \end{bmatrix} = W(x_2, x_3) \begin{bmatrix} x_4 \\ x_5 \\ x_6 \end{bmatrix} \quad (13)$$

where W is as given in Eq. (8) with θ_2 and θ_3 replaced by x_2 and x_3 , respectively, and

$$\begin{bmatrix} \dot{x}_4 \\ \dot{x}_5 \\ \dot{x}_6 \end{bmatrix} = J^{-1} \left\{ D(\delta)u + E \begin{bmatrix} x_4 \\ x_5 \\ x_6 \end{bmatrix} - \begin{bmatrix} x_4 \\ x_5 \\ x_6 \end{bmatrix} \times J \begin{bmatrix} x_4 \\ x_5 \\ x_6 \end{bmatrix} + T_n(t) + G \begin{bmatrix} x_1 \\ x_2 \\ x_3 \end{bmatrix} \right\} \quad (14)$$

and

$$\begin{bmatrix} \dot{x}_7 \\ \dot{x}_8 \\ \dot{x}_9 \\ \dot{x}_{10} \\ \dot{x}_{12} \\ \dot{x}_2 \end{bmatrix} = \begin{bmatrix} u_1 \\ u_2 \\ u_3 \\ u_4 \\ u_5 \\ u_6 \end{bmatrix} \quad (15)$$

Equations (13-15) are of the general form

$$\dot{x} = f(x, u, t) \quad (16)$$

Expanding Eq. (16) about the nominal operating point, x_{nom} and u_{nom} , in a Taylor series for \dot{x} yields

$$\begin{aligned} \dot{x} = & f(x_{nom}, u_{nom}, t) + \left. \frac{\partial f}{\partial x} \right|_{\substack{x=x_{nom} \\ u=u_{nom}}} (x - x_{nom}) \\ & + \left. \frac{\partial f}{\partial u} \right|_{\substack{x=x_{nom} \\ u=u_{nom}}} (u - u_{nom}) + g(x - x_{nom}, u - u_{nom}, t) \end{aligned} \quad (17)$$

where g contains the higher order terms of the series expansion. Defining

$$y = x - x_{nom}, \quad v = u - u_{nom} \quad (18)$$

the general form of the linearized equations is

$$\dot{y} = Ay + Bv \quad (19)$$

where

$$A = \left. \frac{\partial f}{\partial x} \right|_{\substack{x=x_{nom} \\ u=u_{nom}}}, \quad B = \left. \frac{\partial f}{\partial u} \right|_{\substack{x=x_{nom} \\ u=u_{nom}}}$$

The steady state gimbal rate, u_{nom} , is obtained as the equilibrium solution of Eq. (1), (i.e. $\dot{\Omega} = \Omega = 0$), as

$$u_{nom} = -D^{-1}(T_n + G\theta) \quad (20)$$

where D^{-1} is the pseudoinverse of the nonsquare matrix D , and u_{nom} is considered as constant since the time constants of the gravity gradient torques are large compared to the time constants of the stabilized control system. This choice of u_{nom} is not unique, although it is the minimum norm solution, but

it is a commonly used result for cases such as are being considered.

It is desirable to keep the average attitude and attitude rate errors small, as well as to prevent excessive peak errors in attitude and attitude rate. Therefore, the performance measure employed in the optimal control law penalizes position and rate terms to avoid excessively large control effort. Since gimbal stops are not considered here, there is no reason to penalize the gimbal angles. Since $\Omega_{nom} = 0$, the performance measure considered for the optimal control law can be written as

$$J = \int_0^T \frac{1}{2} \{ y^T Q y + v^T R v \} dt \quad (21)$$

where

$$\begin{bmatrix} L_{3 \times 3} & O_{3 \times 3} & O_{3 \times 6} \\ O_{3 \times 3} & J_{3 \times 3} & O_{3 \times 6} \\ O_{6 \times 3} & O_{6 \times 3} & O_{6 \times 6} \end{bmatrix} \quad (22)$$

and R is a diagonal matrix, $r_{ii} > 0$.

The general term $\Omega^T J \Omega$ represents the vehicle kinetic energy and minimizing the integral of the vehicle kinetic energy conserves vehicle energy expenditure. The elements of the L and R matrices are generally chosen smaller than elements of J because of this aspect of energy conservation. It is well known⁹ that the solution to Eq. (21) is of the form

$$\dot{v} = -R^{-1} B^T K y \quad (23)$$

where R is the positive definite (p.d.) control vector weighting matrix, Q is the positive semi-definite (p.s.d) state vector weighting matrix, $T \rightarrow \infty$, and $y(T)$ is unspecified, and K is the symmetric, positive definite gain matrix that is the solution to the matrix Riccati equation

$$\dot{K} = -KA - A^T K - Q + KBR^{-1}B^T K \quad (24)$$

with boundary condition $K(T) = 0$.

Equations (23) and 24) give the optimal solution if the system given by Eq. (19) is completely controllable. If the system is not completely controllable, the solution is optimal only when the uncontrollable states are stable and not penalized. It should be noted that there are techniques for obtaining optimal control solutions without solving the Riccati equation.¹⁰

The solution of the linear regulator problem is an accurate solution to the nonlinear plant if the linearized model is updated frequently enough. The linearized model must be updated as a function of time, gimbal angles, and vehicle attitude commands. The gimbal angles will be the fastest to change and usually can provide the criterion for updating the linearized model. Equations (23) and (24) give a suboptimal solution as a result of the frequent updating of the linearized model, but if the updating period is short compared to the system time constants, then this solution approaches the optimal. An implementation of this suboptimal control system is shown in Fig. 3.

A difficulty in implementing the optimal steering law described by Eqs. (23) and (24) centers about finding the steady-state solution to the matrix Riccati equation, Eq. (24). Problems encountered are excessive computation time, solution accuracy and computational storage burden. Only the first two topics are explored in this paper. Two basic approaches are considered. First, a sensitivity analysis of the gains with respect to the gimbal angles is performed to determine if some of the elements of the gain matrix K may be considered constant. Those gains which may be considered constant would not have to be computed at each linearization update, thus saving on computation time. Second, different solution techniques are evaluated with respect to computation time and accuracy to determine which solution method is most acceptable with respect to these requirements.

III. Riccati Equation Sensitivity Analysis

When the gimbal angles are not penalized, as in the present study, it is often sufficient in practice⁶ to consider only a reduced order system of Eq. (23). Such a reduced sixth-order equivalent of Eq. (23) is

$$\begin{bmatrix} \dot{x}_{1-3} \\ \dot{x}_{4-6} \end{bmatrix} = \begin{bmatrix} 0 & W \\ 0 & A_I \end{bmatrix} \begin{bmatrix} x_{1-3} \\ x_{4-6} \end{bmatrix} + \begin{bmatrix} 0 \\ B_I \end{bmatrix} u \quad (25)$$

where W is given in Eq. (8)

$$\begin{bmatrix} 0 & H_z & H_y \\ -H_z & 0 & H_x \\ H_y & -H_x & 0 \end{bmatrix} \quad (26)$$

$$B_I = J^{-1}D \Big|_{x=x_{nom}} \quad (27)$$

and J is the inertia dyadic of the vehicle.

Rewriting Eq. (24) in the steady state and showing explicit dependence on a parameter α yields

$$A^T(\alpha)K(\alpha) + K(\alpha)A(\alpha) - K(\alpha)S(\alpha)K(\alpha) + Q = 0 \quad (28)$$

where $S(\alpha) = B(\alpha)R^{-1}B^T(\alpha)$. Taking the partial derivative of Eq. (28) with respect to α yields

$$\begin{aligned} \frac{\partial A^T}{\partial \alpha} K + A^T \frac{\partial K}{\partial \alpha} + \frac{\partial K}{\partial \alpha} A + K \frac{\partial A}{\partial \alpha} \\ - \frac{\partial K}{\partial \alpha} SK - K \frac{\partial S}{\partial \alpha} K - KS \frac{\partial K}{\partial \alpha} = 0 \end{aligned} \quad (29)$$

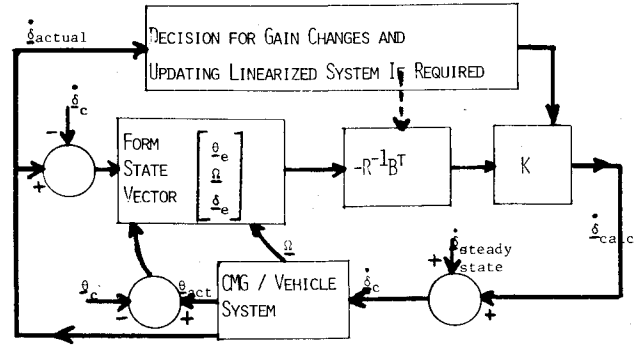


Fig. 3 Suboptimal controller implementation.

Combining like terms simplifies Eq. (29) to

$$\frac{dK}{d\alpha} (A - SK) + (A - SK)^T \frac{dK}{d\alpha} = -K\eta - \eta^T K + K\delta K \quad (30)$$

where $\eta = dA/d\alpha$, $\delta = dS/d\alpha$, and all matrices are evaluated at $\alpha = \alpha_0$. Note that Eq. (30) is in the form

$$FG + G^T F + H = 0 \quad (31)$$

where $F = dK/d\alpha$, $G = A - SK$, and $H = K\eta + \eta^T K - K\delta K$.

An algorithm is given in Ref. 11 that solves equations of the form of Eq. (31) numerically. The steady state Riccati solution for several initial gimbal angle configurations, $K(\alpha_0)$, is computed; then Eq. (31) is iteratively solved for $dK/d\alpha$ using Kleinman's algorithm in Ref. 11. The percentage variation in K for a $\Delta\alpha$ change in a gimbal angle is approximated as

$$\left(S_{\alpha}^K \right)_{ij} = \left(\frac{dK}{d\alpha} \right)_{ij} \frac{\Delta\alpha}{K_{ij}} \quad i, j = 1, 2, \dots, 6 \quad (32)$$

where K_{α}^K is the sensitivity of K with respect to parameter α , α is a gimbal angle, $\alpha = \delta_1, \delta_2, \dots, \delta_6$, and $\Delta\alpha$ is the incremental change in the gimbal angle α .¹² Performing these

Table 1 Range of off-diagonal elements of K

K_{ij}	Range	
	Max	Min
K_{12}	1.75×10^4	-4.32×10^4
K_{13}	5.27×10^3	-4.30×10^4
K_{14}	2.51×10^5	1.55×10^5
K_{15}	6.09×10^4	-1.51×10^5
K_{16}	1.91×10^4	-1.49×10^5
K_{23}	4.34×10^4	-8.03×10^4
K_{24}	6.14×10^4	-1.49×10^5
K_{25}	1.60×10^6	1.28×10^6
K_{26}	1.55×10^5	-2.86×10^5
K_{34}	1.83×10^4	-1.49×10^5
K_{35}	1.56×10^5	-2.85×10^5
K_{36}	1.84×10^6	1.27×10^6
K_{45}	2.52×10^5	-6.08×10^5
K_{46}	7.84×10^4	-6.06×10^5
K_{56}	6.67×10^5	-1.20×10^6

Table 2 Range of off-diagonal elements of S_{α}^K due to variations in the gimbal angles

S_{α}^K K_{ij}	(Absolute Value)	
	Max	Min
K_{12}	7.77×10^5	4.42×10^{-3}
K_{13}	2.43×10^6	3.05×10^{-1}
K_{14}	9.81	7.74×10^{-4}
K_{15}	2.79×10^4	2.11×10^{-2}
K_{16}	7.36×10	2.73×10^{-1}
K_{23}	4.33×10^4	7.83×10^{-3}
K_{24}	2.39×10^3	1.23×10^{-2}
K_{25}	1.53	2.09×10^{-6}
K_{26}	1.35×10^4	1.54×10^{-2}
K_{34}	9.55×10^3	1.12×10^{-1}
K_{35}	8.41×10^3	5.89×10^{-4}
K_{36}	2.74	1.0×10^{-3}
K_{45}	4.04×10^5	3.23×10^{-3}
K_{46}	1.22×10^8	4.37×10^{-2}
K_{56}	5.79×10^4	1.68×10^{-3}

Table 3 Range of diagonal elements of K

K_{ij}	Range of Matrix Element Values	
	Max	Min
K_{11}	3.83×10^5	3.54×10^5
K_{22}	2.39×10^6	2.30×10^6
K_{33}	2.43×10^6	2.28×10^6
K_{44}	8.89×10^5	5.10×10^5
K_{55}	5.78×10^6	4.41×10^6
K_{66}	6.84×10^6	4.38×10^6

operations for gimbal angle orientations that are combinations of values of gimbal angles between 0° and 30° was sufficient to indicate that no gains were insensitive enough to gimbal angle variations to consider them constant. In addition to the sensitivity expression in Eq. (32), other approaches on both the theory and computation of optimal control system sensitivity include Refs. 13-16.

The diagonal elements of the steady-state solution to the Riccati equation are generally much less sensitive to gimbal angle variations than are the off-diagonal terms. Table 1 gives the range of the values of the off-diagonal terms of the gain matrix for the various gimbal angle configurations that are considered. For these same cases, Table 2 gives the range of the sensitivities of these off-diagonal terms to 5° incremental changes in the δ_i gimbal angle. Results are presented only for the δ_1 gimbal angle because these results are typical of those obtained for the other gimbal angles. It should be noted that the actual maximum sensitivities for these off-diagonal elements are infinite when these gains pass through zero; however, the discrete sampling process employed does not pick up these points. This fact does not invalidate the results of Table 2, however. Specifically, the off-diagonal terms are not insensitive enough to the gimbal angle variations to be considered constant. This same information is conveyed by Table 1 when one observes that the off-diagonal gain values

Table 4 Range of diagonal elements of S_{α}^K due to variations in the gimbal angles

S_{α}^K K_{ij}	Range (Absolute Value)	
	Max	Min
K_{11}	1.30	2.93×10^{-2}
K_{22}	2.93	1.79×10^{-1}
K_{33}	1.47	1.93×10^{-1}
K_{44}	4.66	3.94×10^{-1}
K_{55}	5.86	1.25
K_{66}	4.81	1.27

fluctuate from large *negative* values to large positive values. The additional information gleaned from Table 2 is that for the gimbal angle combinations employed the diagonal gain matrix values are clearly insensitive to gimbal angle variation.

The range of the values of the Riccati gain matrix diagonal terms are given in Table 3 for the different gimbal angle configurations analyzed. Table 4 describes the range of the maximum sensitivities of these gain elements with respect to variations in the six gimbal angles. This table illustrates the diagonal terms are much less sensitive to the gimbal angles than the off-diagonal terms; however, it also indicates that no off-diagonal element of the Riccati gain matrix are insensitive enough to the gimbal angle to be considered constant. *As a consequence, virtually all elements of the gain matrix need to be computed at each linearization update and little computational time can be saved by considering some elements to be constant.*

In addition to determining K variation, the closed-loop root variation due to the optimal feedback law can be studied.¹⁷ Since the feedback system is of the form

$$\dot{z} = Gz + Bu$$

$$u = -R^{-1}B^TKz \quad (33)$$

then the closed loop system is

$$\dot{z} = (G - BR^{-1}B^TK)z \quad (34)$$

$$\dot{z} = \tilde{A}z \quad (35)$$

and the roots of \tilde{A} are those of the total system. In this paper no attempt is made to identify the variation in roots of \tilde{A} because 1) both G and B change form in a complicated manner, and 2) variation in the elements of K are necessary but not sufficient conditions for altering the feedback gains and thus the closed loop roots.

IV. Numerical Solution Techniques for the Riccati Equation

Numerous numerical iteration schemes are available for use in obtaining the steady-state Riccati equation solution, the so-called Algebraic Riccati Equation (ARE). Compared in this section are various integration "shooting-method" and algebraic techniques for the Riccati solution, each of which is briefly described in the following for the basic dynamics $\dot{x} = f(x)$.

Integration Methods

1) 4th-Order Runge-Kutta

$$x(t_{k+1}) \approx x(t_k) + \frac{h}{6} (f_k^A + 2f_k^C + f_k^D) \quad (36)$$

where

$$\begin{aligned} f_k^A &= f[x(t_k), t_k] \\ f_k^B &= f\left[x(t_k) + \frac{h}{2} f_k^A, t_k + \frac{h}{2}\right] \\ f_k^C &= f\left[x(t_k) + \frac{h}{2} f_k^B, t_k + \frac{h}{2}\right] \\ f_k^D &= f[x(t_k) + h f_k^C, t_k + h] \end{aligned}$$

2) Euler

$$x(t_{k+1}) \approx x(t_k) + h f[x(t_k), t_k] \quad (37)$$

3) Modified-Euler

$$x(t_{k+1}) \approx x(t_k) + \frac{h}{2} (f[x(t_k), t_k] + f[P, t_{k+1}]) \quad (38)$$

where

$$P = x(t_k) + h f[x(t_k), t_k]$$

Shooting Methods²⁰

1) Exponential Extrapolation

$$y(t) = C_1 + C_2 e^{-C_3 t} \text{ solution form}$$

$y_1^{(i)}, y_2^{(i)}, y_3^{(i)}$ three points along the transient solution

$$y^{(i)}(t = \infty) = \frac{y_1^{(i)} y_3^{(i)} - y_2^{(i)2}}{y_1^{(i)} + y_3^{(i)} - 2y_2^{(i)}} \quad (39)$$

$$\Delta y^{(i)} = \frac{y_1^{(i)} y_3^{(i)} - y_2^{(i)2}}{y_1^{(i)} + y_3^{(i)} - 2y_2^{(i)}} - y_1^{(i)} \quad (40)$$

2) Constant Proportionality

$$y^{(i+1)} = y^{(i)} \Delta y^{(i)} \quad (41)$$

$y_1^{(i)}, y_2^{(i)}$ two data points Δt seconds apart

$$\Delta y^{(i)} = h \frac{y_2^{(i)} - y_1^{(i)}}{\delta t} \quad (42)$$

h = constant "shooting" factor

Algebraic

1) Kleinman Iterative^{11,21}

$V_k, k=0, 1, 2, \dots$ is the unique positive-definite solution to

$$A_k^T V_k + V_k A_k + Q + L_k^T R L_k = 0 \quad (43)$$

the algorithm is

$$L_k = R^{-1} B^T V_{k-1}; L_0 \text{ chosen so}$$

$$A_0 = A - B L_0 \text{ has negative real eigenvalues}$$

$$A_k = A - B L_k$$

then

$$\lim_{k \rightarrow \infty} V_k = k$$

2) Potter Algebraic^{22,23}

Form

$$H = \begin{bmatrix} A & -B R^{-1} B^T \\ -Q & -A^T \end{bmatrix}_{2n \times 2n} \quad (44)$$

Compute I_i = eigenvector $[H]_i$ corresponding to stable eigenvalues of H . Form

$$\begin{bmatrix} D \\ E \end{bmatrix}_{2n \times 2n} \text{ array of eigenvectors } [I_1, I_2, \dots, I_n] \quad (45)$$

$$K \approx E D^{-1} \quad (46)$$

Euler, Modified Euler, and Runge-Kutta integration procedures are examined in this analysis. Additionally, these solution techniques are examined with exponential acceleration and proportional acceleration, both with and without instability retardation routines. Finally, the Kleinman and Potter algebraic routines are compared to the integration routines. A conventional fourth-order Runge-Kutta integration algorithm is included for comparison purposes. Other studies reporting on computational aspects of the Riccati equation solution include work on the Newton-Raphson approach,^{24,25} eigenvector expansion techniques,²⁶ nonrecursive algebraic solutions,²⁷ analytical methods,²⁸ and iterative algebraic procedures.²⁹

With respect to integration algorithms, the Euler and Modified-Euler are considered and compared to the conventional fourth-order Runge-Kutta to determine if other algorithms might yield solutions to K in Eq. (24) with less computation time but comparable accuracy.

The acceleration (shooting-method) techniques²⁰ are applicable when: 1) only the steady-state solution is desired; 2) the boundary conditions and internal constraints are either constant or cyclic; and 3) the steady-state results are independent of the initial conditions.

There are two accelerations techniques—exponential extrapolation and constant proportionality adjustment. Exponential extrapolation involves fitting and exponential curve through three points in the transient solution and predicting the steady-state value. The constant proportionality adjustment is

$$\Delta Y = \text{SKIP} \left[\frac{(Y_2 - Y_1)}{\Delta t} \right] \quad (47)$$

where SKIP is a constant multiplication factor input by the user. This method is usually less accurate than exponential extrapolation, but it usually requires less computation time (as well as requiring less computer storage space).

Since the possibility of solution instability is enhanced with the accelerated integration techniques, the sign of the adjustment to the gain values can be checked. If the sign changes, then the incremental adjustment is modified by a constant reduction factor to prevent instability or at least to retard it. If the sign change is indicative of a simple overshoot rather than instability, the modification to the incremental adjustment should speed up the solution computationally.

A program for the Linear Quadratic Loss (LQL) problem²² uses Potter's algebraic method²³ to obtain the steady-state solution to the Riccati equation. Potter's method involves finding the eigenvectors (or pseudo-eigenvectors) corresponding to eigenvalues with negative real parts of the $2n \times 2n$ Hamiltonian matrix given by Eq. (44). Spectral factorization of the Hamiltonian matrix is used to obtain these eigenvalues. The stable eigenvectors are then used to form a $2n \times 2n$ matrix whose columns are the real eigenvectors. If the eigenvectors are in complex conjugate pairs, two vectors made up of the real and imaginary parts of one of the complex eigenvectors are used instead of the complex entries. If this $2n \times n$ matrix

Table 5 Computation time and accuracy comparison for the Runge-Kutta Method

Δt	Normalized Accuracy	Normalized Computational Time
-.0001	*	*
-.005	*	*
-.01	*	*
-.05	2.79	36.17
-.1	1.59	17.86
-.5	.14	3.19

Table 6 Comparison of integration methods ($\Delta t = -0.5$)

Solution Method	Normalized Accuracy (From (43))	Normalized Computation Time	Normalized T + Acc.
Runge-Kutta	.14	3.19	3.33
Runge-Kutta (Instability Suppression)	.14	3.23	3.37
Modified Euler	.07	2.91	2.98
Modified Euler (Instability Suppression)	.17	2.23	2.40
Euler	0	.08	.08
Euler (Instability Suppression)	.10	7.77	7.87

Table 7 Comparison of standard Euler and linearly accelerated Euler integration solutions for K

Algorithm	Δt	Normalized Accuracy	Computational Time	Equal Weighting of Time and Accuracy
Euler	-.1	1.01	3.54	4.55
Euler	-.05	2.98	8.22	11.19
Euler	-.01	29.65	34.58	64.23
Acc Euler	-.1	.08	3.05	3.14
Acc Euler	-.05	1.93	2.51	4.43
Acc Euler	-.01	32.04	12.41	44.44

Table 8 Comparison of computation time for solution techniques

Algorithm	Δt	Normalized Computational Time
Potter's Algebraic	*	0
Euler	-.5	.08
Euler (Linear Acceleration)	-.1	1.65
Modified Euler	-.5	2.23
Euler (Linear Acceleration)	-.05	2.51
Runge-Kutta (for comparison)	-.5	3.19

so formed is Eq. (45), then the steady-state solution to Eq. (24) is given by Eq. (46).

Using the same system parameters as in Refs. 6 and 8, solution to the Riccati equation are obtained using the previous algorithms. *Since the algorithms would be programmed on a particular flight control computer, the actual computation times for these procedures would be meaningless since computations times vary greatly for different computer configurations.* Therefore, the tabular results presented in the remainder of this section are normalized. The minimum value

Table 9 Solution methods yielding best accuracy

Algorithm	Δt	Normalized Accuracy
Euler	-.5	0
Modified Euler	-.5	.07
Euler (Linear Acceleration)	-.1	.08
Euler (Instability Suppression)	-.5	.10
Runge-Kutta	-.5	.14
Kleinman Iterative	*	.17

of the parameter for all cases considered is assigned the value zero while the maximum value is assigned the value of 100. All intermediate values are assigned a value between 0 and 100 in the following linear fashion

$$p_n = \frac{(p_i - p_{\min})}{(p_{\max} - p_{\min})} 100 \quad (48)$$

where p_n is the normalized parameter value, p_i is the actual parameter value, p_{\min} is the minimum parameter value, p_{\max} is the maximum parameter value.

Since the steady-state solution to the Riccati equation is desired, the derivatives of each of the gains at the computed solution point gives a measure of the solution accuracy. For the results included in the remainder of this section, the accuracy comparison values are obtained by summing the absolute values of all the elements of the gain derivative matrix, i.e.

$$L = -KA - A^T K - Q + KBR^{-1}B^T K \quad (49)$$

$$P = \sum_{i=1}^n \sum_{j=1}^n |l_{ij}| \quad n = \text{system order} \quad (50)$$

These values of P are then normalized according to Eq. (48).

The integration routines are very sensitive to the integration time increment. Table 5 illustrates the expected decrease in computational time for an increase in the integration time increment for the conventional fourth-order Runge-Kutta integration routine.

For those cases including instability suppression, the value of the constant factor to modify the solution adjustment was selected to be $\Delta t = -0.1$. This value represents a compromise between accuracy and time. Solutions to the Riccati equations were obtained using other values, but there was no general trend. In some instances -0.1 gave the better result with respect to computational time and accuracy, while in other instances -0.025 and -0.25 gave better results. Table 6 compares the three integration methods to each other with and without instability suppression. The instability suppression has a more noticeable effect on the Euler and Modified Euler routines. If computational time and accuracy are weighted equally as in Table 6, then the Euler algorithm accomplishes the desired results more efficiently.

The exponential acceleration of the integrated solutions yielded poor results, indicating that the transient solution for the system studied is not approximated by an exponential very well. Consequently, either the solution tends toward instability or requires a prohibitive computation time when instability suppression is included.

The linearly accelerated integration algorithms are sensitive to the value of the constant of proportionality used to accelerate the solution. If this constant is chosen too large, this procedure will also result in unstable solutions or prohibitive computation times if instability suppression is used. Table 7

Table 10 Solution methods providing the best computation time-accuracy tradeoff

Algorithm	Δt	Normalized Weighting of Accuracy and Comp. Time
Euler	-.5	.08
Potter's Method	*	.95
Euler (Linear Acceleration)	-.1	2.22
Modified Euler	-.5	2.40
Euler (Linear Acceleration)	-.05	3.28

Table 11 Algebraic techniques compared with integration routines ($\Delta t = -0.05$)

Algorithm	Normalized Accuracy	Normalized Computational Time	Normalized Accuracy and Time Weighting
Runge Kutta	.14	3.19	3.33
Euler	0	.08	.08
Potter's Method	.95	0	.95
Kleinman Iterative	.17	15.76	15.94

provides a comparison of some solutions to Eq. (24) obtained by Euler and linearly accelerated by Euler integration. The linearly accelerated routine yields slightly better results than the simple Euler integration routine. For a particular system, a value for the constant proportion adjustment can be obtained empirically. This must be done to minimize the possibility of unstable solutions.

For all solution techniques considered, Table 8 presents those algorithms requiring the least computational time, Table 9 those techniques giving the most accurate solutions, and Table 10 the best solution techniques considering equal weighting of time and accuracy. The Euler integration routine with a step-size of -0.5 gives the best results of the algorithms employed to solve the Riccati equation.

Table 11 compares the two algebraic techniques with the Euler integration solution because the integration solutions have the property that the numerical solution goes unstable if the step-size is chosen to be too large. In contrast, larger step-sizes give better accuracy and computational time tradeoffs. This is not true for the algebraic techniques so that, depending on the applications, it may be desirable to use the less efficient algebraic algorithms.

V. Summary and Conclusions

From a study of the results in Sec. III, it is clear that 1) it is not feasible to eliminate off-diagonal Riccati equation terms in the update equation, Eq. (19), for the system studied due to their high sensitivity as shown in Tables 2-4; and 2) some diagonal elements could be held constant; however it is the elimination of the $n(n-1)/2$ off-diagonal terms of an n th order system, which offers the significant time and storage advantages.

From Sec. IV, various solution methods offer a "best" tradeoff for the steady-state Riccati equation. From the tabulated results, it can be seen that 1) Potter's Algebraic technique requires the least computation time of the methods studied, 2) the simple Euler method yielded the best overall accuracy; and 3) the simple Euler method yielded the best results when accuracy and computation time were equally weighted.

Whether one uses a full state variable formulation, a reduced-order system, or simple steering laws depends on the particular application and the response specifications.³⁰ However, for the class of spacecraft using CMG's for attitude control, it appears from the present study as well as Ref. 6

that if an optimal linear regulator formulation is employed, a full Riccati equation solution of $n(n+1)/2$ elements of K is required to be computed at each update cycle.

Acknowledgement

This work was sponsored in part under NASA Contract NAS8-26580.

References

- ¹Chubb, W. and Epsten, M., "Application of Control Moment Gyros in the Attitude Control of the Apollo Telescope Mount," AIAA Paper 68-866, Pasadena, Calif., 1968.
- ²Liu, T. C., et al., "Optimal Control of a Variable Spin Speed CMG System for Space Vehicles," *Proceedings of the IEEE Conference on Decision and Control*, Dec. 1973, pp. 722-726.
- ³Kuo, B. et al., "Stability Analysis of the Discrete-Data Large-Space-Telescope System," *Journal of Spacecraft and Rockets*, Vol. 13, June 1976, pp. 332-339.
- ⁴Kalman, R. E., "On the General Theory of Control Systems," *Proceedings of First IFAC Congress*, International Federation on Automatic Control, 1960, pp. 481-493.
- ⁵White, L. R., Colburn, B. K., and Boland, J. S., "Some Basic Approaches to Optimal CMG Steering Laws Requiring No Riccati Equation Computations," *Proceedings of the Seventh Annual Southeastern Symposium on System Theory*, Auburn University, Auburn, Alabama, March 1975.
- ⁶Skelton, R. E., "Optimal Momentum Management in Momentum Exchange Control Systems for Orbiting Vehicles," Sperry Rand, Huntsville, Ala., Rep. No. SP-230-0252, Sept. 1969.
- ⁷White, L. R., Colburn, B., and Boland, J., "Design Analogy Between Optimal Time-Fuel and Rate-Ledge Relay Controllers," *Journal of Spacecraft and Rockets*, Vol. 13, April 1976, pp. 214-219.
- ⁸White, L. R., "Some Optimal Considerations in Attitude Control Systems," M. S. Thesis, Department of Electrical Engineering, Auburn University, Auburn, Alabama, 1973.
- ⁹Kirk, D. E., *Optimal Control Theory*, Prentice-Hall, Englewood Cliffs, N. J., 1970, pp. 209-219.
- ¹⁰Ramani, N., "A Note on the Single-Input Optimal Regulator Problem," *IEEE Transactions Automatic Control*, Vol. AC-21, June 1976, pp. 430-431.
- ¹¹Kleinman, D. L., "An Iterative Technique for Riccati Equation Computations," Bolt, Beranek, and Newman, Inc., Cambridge, Mass., Technical Memorandum No. DLK-1, June 1970.
- ¹²Jamshidi, M., D'Ans, G. C., and Kokotovic, P., "Application of a Parameter-Imbedded Riccati Equation," *IEEE Transactions on Automatic Control*, Vol. AC-15, pp. 682-683, Dec. 1970.
- ¹³Sobral, M., "Sensitivity in Optimal Control Systems," *Proceedings of the IEEE*, Vol. 56, Oct. 1968, pp. 1644-1651.
- ¹⁴Perkins, W. and Cruz, J., "The Parameter Variation Problem in State Feedback Control Systems," *Transactions ASME: Journal of Basic Engineering*, Series D, Vol. 87, 1965, pp. 120-124.
- ¹⁵Bartels, R. and Stewart, G., "Solution of the Matrix Equation $AX + XB = C$," *Communications of the ACM*, Vol. 15, Sept. 1972, pp. 820-826.
- ¹⁶Graupe, D., "Optimal Linear Control Subject to Sensitivity Constraints," *IEEE Transactions of Automatic Control*, Vol. AC-19, Oct. 1974, pp. 593-594.
- ¹⁷Kwakernaak, H., "Asymptotic Root Loci of Multivariable Linear Optimal Regulators," *IEEE Transactions on Automatic Control*, Vol. AC-21, June 1976, pp. 378-382.
- ¹⁸Athans, M., et al., *Systems, Networks, and Computation: Multivariable Methods*, McGraw-Hill, N. Y., 1974, pp. 469-475.
- ¹⁹James, et al., *Applied Numerical Methods*, International Printing, 1970, pp. 326-339.
- ²⁰Russell, D. J., "Computer Program to Accelerate Transient Finite-Difference Solutions to Steady-State," *Third Annual Houston Conference on Computer and System Science*, pp. 291-301, 1971.
- ²¹Kleinman, D. L., "On an Iterative Technique for Riccati Equation Computations," *IEEE Transactions on Automatic Control*, Vol. AC-13, Feb., 1968, pp. 114-115.
- ²²Bullock, T. E and Fosha, C. E., "A General Purpose Program for Estimation, Control, and Simulation," *Proceedings of Eighth Annual IEEE Region III Convention*, Huntsville, Alabama, Nov. 19-21, 1969, pp. 102-107.
- ²³Potter, J., "Matrix Quadratic Solutions," *SIAM Journal on Applied Mathematics*, Vol. 14, May 1966.
- ²⁴Sandell, N., "On Newton's Method for Riccati Equation Solution," *IEEE Transactions on Automatic Control*, Vol. AC-19, June 1974, pp. 254-255.

²⁵Man, F., "Numerical Solution of the Algebraic Matrix Riccati Equation," *Proceedings of the IEEE Decision and Control Conference*, Dec. 1973, pp. 549-553.

²⁶Fath, A., "Computational Aspects of the Linear Optimal Regulator Problem," *IEEE Transactions on Automatic Control*, Vol. AC-14, Oct. 1969, pp. 547-550.

²⁷Vaughan, D., "A Nonrecursive Algebraic Solution for the Discrete Riccati Equation," *IEEE Transactions on Automatic Control*, Vol. AC-15, Oct. 1970, pp. 597-599.

²⁸Shubert, H., "An Analytic Solution for an Algebraic Matrix Riccati Equation," *IEEE Transactions on Automatic Control*, Vol. AC-20, April 1975, pp. 255-256.

²⁹Meyer, G. and Payne, H., "An Iterative Method of Solution of the Algebraic Riccati Equation," *IEEE Transactions on Automatic Control*, Vol. AC-17, Aug. 1972, pp. 550-551.

³⁰White, L. R., Colburn, B. K. and Boland, J. S., "Some Simple CMG Steering Laws for Spacecraft Attitude Control Systems," *Proceedings of the Ninth Asilomar Conference on Circuits and Systems*, Pacific Grove, Calif., Nov. 1975, pp. 598-604.

From the AIAA Progress in Astronautics and Aeronautics Series

SPACECRAFT CHARGING BY MAGNETOSPHERIC PLASMAS—v. 47

Edited by Alan Rosen, TRW, Inc.

Spacecraft charging by magnetospheric plasma is a recently identified space hazard that can virtually destroy a spacecraft in Earth orbit or a space probe in extra terrestrial flight by leading to sudden high-current electrical discharges during flight. The most prominent physical consequences of such pulse discharges are electromagnetic induction currents in various on-board circuit elements and resulting malfunctions of some of them; other consequences include actual material degradation of components, reducing their effectiveness or making them inoperative.

The problem of eliminating this type of hazard has prompted the development of a specialized field of research into the possible interactions between a spacecraft and the charged planetary and interplanetary mediums through which its path takes it. Involved are the physics of the ionized space medium, the processes that lead to potential build-up on the spacecraft, the various mechanisms of charge leakage that work to reduce the build-up, and some complex electronic mechanisms in conductors and insulators, and particularly at surfaces exposed to vacuum and to radiation.

As a result, the research that started several years ago with the immediate engineering goal of eliminating arcing caused by flight through the charged plasma around Earth has led to a much deeper study of the physics of the planetary plasma, the nature of electromagnetic interaction, and the electronic processes in currents flowing through various solid media. The results of this research have a bearing, therefore, on diverse fields of physics and astrophysics, as well as on the engineering design of spacecraft.

304 pp., 6 x 9, illus. \$16.00 Mem. \$28.00 List

TO ORDER WRITE: Publications Dept., AIAA, 1290 Avenue of the Americas, New York, N. Y. 10019